



Highly oriented ferroelectric CaBi₂Nb₂O₉ thin films deposited on Si(100) by pulsed laser deposition

S. B Desu, H. S Cho, and P. C. Joshi

Citation: [Applied Physics Letters](#) **70**, 1393 (1997); doi: 10.1063/1.118587

View online: <http://dx.doi.org/10.1063/1.118587>

View Table of Contents: <http://scitation.aip.org/content/aip/journal/apl/70/11?ver=pdfcov>

Published by the [AIP Publishing](#)

Articles you may be interested in

[Metal-ferroelectric \(BiFeO₃ \)-insulator \(Y₂O₃ \)-semiconductor capacitors and field effect transistors for nonvolatile memory applications](#)

Appl. Phys. Lett. **94**, 142905 (2009); 10.1063/1.3114403

[Forming gas annealing on physical characteristics and electrical properties of Sr_{0.8}Bi₂Ta₂O₉/Al₂O₃/Si capacitors](#)

J. Appl. Phys. **94**, 1877 (2003); 10.1063/1.1588362

[Enhanced ferroelectric properties in laser-ablated SrBi₂Nb₂O₉ thin films on platinized silicon substrate](#)

Appl. Phys. Lett. **81**, 1672 (2002); 10.1063/1.1502440

[CaBi₂Ta₂O₉ ferroelectric thin films prepared by pulsed laser deposition](#)

Appl. Phys. Lett. **78**, 2925 (2001); 10.1063/1.1370545

[Properties of SrBi₂Ta₂O₉ ferroelectric thin films prepared by a modified metalorganic solution deposition technique](#)

Appl. Phys. Lett. **70**, 1080 (1997); 10.1063/1.118485



Re-register for Table of Content Alerts

Create a profile.



Sign up today!



Highly oriented ferroelectric $\text{CaBi}_2\text{Nb}_2\text{O}_9$ thin films deposited on Si(100) by pulsed laser deposition

S. B. Desu, H. S. Cho, and P. C. Joshi

Department of Materials Science and Engineering, Virginia Polytechnic Institute and State University, Blacksburg, Virginia 24061-0237

(Received 15 November 1996; accepted for publication 7 January 1997)

We report the successful deposition of highly c -axis oriented $\text{CaBi}_2\text{Nb}_2\text{O}_9$ (CBN) thin films directly on p -type Si(100) substrates by pulsed laser deposition. The CBN thin films exhibited good structural, dielectric, and CBN/Si interface characteristics. The electrical measurements were conducted on CBN thin films in a metal-ferroelectric-semiconductor (MFS) capacitor configuration. The typical measured small signal dielectric constant and the dissipation factor at a frequency of 100 kHz were 80 and 0.051, respectively. The leakage current of the MFS capacitor structure was governed by the Schottky barrier conduction mechanism and the leakage current density was lower than 10^{-7} A/cm² at an applied electric field of 100 kV/cm. The capacitance-voltage measurements on MFS capacitors established good ferroelectric polarization switching characteristics. © 1997 American Institute of Physics. [S0003-6951(97)00711-0]

Ferroelectric thin films have been widely investigated for their use in a variety of devices exploiting their unique piezoelectric, pyroelectric, polarization switching, and electro-optic properties.¹ Integration of these films directly with Si or poly-Si will open a new era for practical applications in both active and passive electronic devices. Recently, there has been a surge in research activity on ferroelectric thin films for nonvolatile random access memory (NVRAM) applications. Ferroelectric thin films with large remanent polarization, low coercive field, low fatigue rate, and good retention characteristics have the potential for use as memory elements in high density 1T-1C nonvolatile memories.² The ferroelectric gate insulator field effect transistor is the desired configuration for a one transistor high density memory array. Metal-ferroelectric-semiconductor field effect transistors (MFSFETs) have attracted considerable attention as promising devices for applications to nonvolatile memories. MFSFET exploits the ferroelectric field effect, which is the modulation of conductivity by the electrostatic charges induced by ferroelectric polarization, and thus requires the direct deposition of ferroelectric thin film on Si wafer. For use in MFSFET, the ferroelectric film need not have a high remanent polarization; it should have just sufficient polarization to cause modulation of the FET channel conductivity. Additionally, it is necessary that the film maintains its ferroelectric properties on the semiconductor surface and the interface state density at the ferroelectric film/Si interface be small enough for the normal MOSFET operation. Thin films of various ferroelectric materials have been investigated for MFSFET devices. Thin films of these materials usually exhibit good ferroelectric properties on metal electrodes such as platinum. However, it is difficult to preserve ferroelectricity on Si due to existence of interfacial traps and/or interdiffusion of the constituent elements. Therefore, there are a few reports of good MFS devices. In the present letter, we report the fabrication of highly oriented $\text{CaBi}_2\text{Nb}_2\text{O}_9$ (CBN) thin films directly on Si by pulsed laser deposition technique. The Pt/CBN/Si capacitors exhibited the desired polarization switching behavior; establishing good CBN/Si interface characteristics.

CBN is a layered perovskite ferroelectric oxide, whose lattice constants are: $a=0.5435$ nm, $b=0.54658$ nm, and $c=2.4970$ nm.³ The CBN material was selected because of its good lattice matching with Si substrate, reasonably high dielectric constant, and low intrinsic defect density of layered perovskite structure. The CBN thin films are very likely to grow on Si(100) with a highly preferred (001) orientation since they have a very good lattice matching along a - and b -axis with Si(100). For device applications, a single crystalline film has an edge over a polycrystalline film in obtaining stable and desirable properties. In this letter, we report the structural and electrical characteristics of highly c -axis oriented $\text{CaBi}_2\text{Nb}_2\text{O}_9$ (CBN) thin films deposited on Si by pulsed laser deposition (PLD) technique. The $\text{CaBi}_2\text{Nb}_2\text{O}_9$ thin films were deposited on p -type ($\rho\sim 30$ Ω cm) Si(100) substrates by a pulsed laser ablation technique. A Lambda Physik (LPX) 300 excimer laser utilizing KrF radiation (248 nm) was used at a pulse rate of 4 Hz and a laser energy of 700 mJ. The film growth rate was 0.17 nm/s. The target having the stoichiometric composition was prepared by a conventional ceramic process. The calcination and sintering were conducted in air at temperatures of 900 and 1120 °C for 3 h, respectively. The substrates were cleaned by a room temperature technique called spin etching,⁴ to remove the native silicon oxide and make the substrate surface hydrogen terminated. Substrates were placed parallel to the target at a distance of 60 mm. During deposition, the chamber pressure was maintained at 200 mTorr with oxygen gas, and the target and the substrates were rotated at a speed of 11 and 4 rpm, respectively. The crystallographic structure of the as-deposited films was investigated by x-ray diffraction (XRD) utilizing CuK_α radiation. Surface and cross-sectional morphologies of the films were observed by atomic force microscopy (AFM) and scanning electron microscopy (SEM). The thickness of the films was measured by spectroscopic ellipsometry and cross-sectional SEM. Several platinum electrodes (contact area= 5.6×10^{-4} cm²) were sputter deposited through a mask on the top surface of the films to form metal-ferroelectric-semiconductor (MFS) capacitors. The capacitance-voltage ($C-V$) measurements were conducted

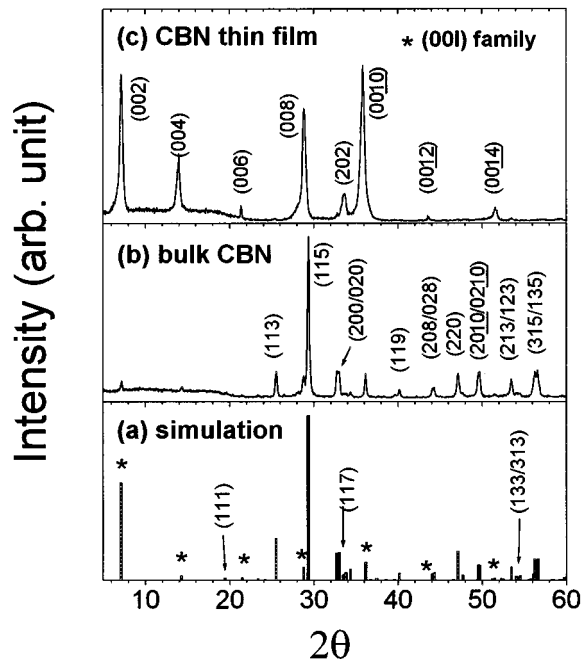


FIG. 1. Comparison of XRD patterns: (a) simulated $\text{CaBi}_2\text{Nb}_2\text{O}_9$ pattern, (b) bulk $\text{CaBi}_2\text{Nb}_2\text{O}_9$ (target), and (c) $\text{CaBi}_2\text{Nb}_2\text{O}_9$ thin film on *p*-type Si(100) showing (001) preferred orientation.

on MFS capacitors at room temperature with a HP 4192A impedance analyzer.

Figure 1 shows the XPD patterns of (a) simulated CBN, (b) bulk CBN (target), and (c) as-deposited CBN thin film. The simulated pattern was generated, based on an orthorhombic crystallographic structure, by XPOWLOT software developed by Gibbs *et al.*⁵ The space group used was Cmc_2_1 (an international type), which was transformed from the A_2_1am reported by Newnham *et al.*⁶ with a proper transforming matrix. The XRD pattern of the target [Fig. 1(b)] matched quite well with the simulated pattern [Fig. 1(a)] except for the intensity of the (002) peak, which implied that the target used was a single phase of CBN and the simulated pattern was an acceptable result. Since there are no reports on the XRD patterns of CBN, these might be used as standard data. Figure 1(c) shows a typical XRD pattern of the highly *c*-axis oriented CBN thin films, where most of the peaks are in the (001) family. The pole figure measurement also revealed that the films had a highly (001) preferred orientation. The ω -scan measurement showed that the full-width at half-maximum of the (0010) peak was 4.00° . The (001) preferred orientation of the CBN thin films on Si(100) is believed to be due to good lattice matching between CBN and Si.

Figure 2 shows the typical AFM micrographs of the highly oriented CBN thin films. Figure 2(a) is a normal height image obtained in a tapping mode AFM where the oscillation amplitude is used as a feedback signal, and Fig. 2(c) shows a relationship between the height and the color of the grains. The film consisted of large grains of about 300 nm in diameter and small grains of about 50 nm in diameter. The size of the large grains was slightly larger than the film thickness, implying that the growth behavior of each large

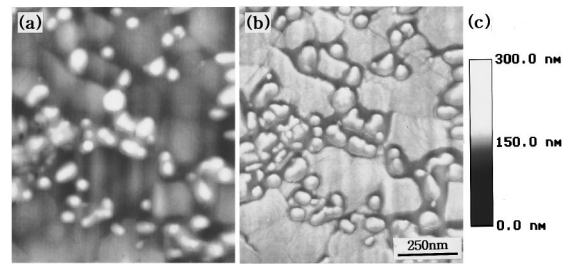


FIG. 2. Typical AFM micrographs of the $\text{CaBi}_2\text{Nb}_2\text{O}_9$ thin film showing (001) preferred orientation: (a) height image, (b) phase image, and (c) the scale bar showing the relationship between the height and the color of the grains.

grain was similar to an epitaxial growth. The top of the small grain was higher than that of the large grain by more than 100 nm. The difference in height appears to be due to renucleation during deposition. The large grains are grown from the initial stage of film growth and they have enough time to grow in the direction parallel as well as perpendicular to the substrate to become large grains, while the small grains, which renucleated and survived on top of the large grains, grow faster than the large grains in the direction perpendicular to the substrate.

The grain morphology of the film is better shown in the AFM phase image as shown in Fig. 2(b). The phase image is obtained by an extender electronics module where the phase lag of the cantilever oscillation relative to the signal sent to the cantilever's piezo driver is used as a feedback signal. It is clear from Fig. 2 that the large grains did not have a spherical shape, whereas the small grains had a spherical shape. Thus, the radius of curvature of the small grains is much smaller than that of the large grain. This implies that the small grains had higher activity than the large grains ($\alpha = 2\gamma/r$, where α : activity of grain, γ : surface energy, and r : radius of curvature), and thus small grains were growing faster than the large grain. The phenomenon matches well with the fact that the top of the small grains was higher than that of the large grains.

Figure 3 shows the leakage current density versus electric field ($J-E$) characteristics of the MFS structure. The CBN thin films on Si exhibited good leakage current characteristics. A strong polarity dependence of the leakage current was observed since the top and bottom electrodes were different. The polarity dependence was caused by the different Schottky barrier height at the interfaces between electrodes and film. In addition, a $\log J$ vs $E^{1/2}$ plot showed a straight line behavior at high voltages indicating that the conduction in high voltage range was controlled by the Schottky barrier. The leakage current was much lower when a positive voltage was applied to the top electrode as compared to negative voltage. This appeared to be due to the formation of a depletion layer near the interface at positive bias voltages, as well as the difference in the Schottky barrier height between both the interfaces. The leakage current density was lower than 10^{-7} A/cm^2 up to an applied electric field of 100 kV/cm; establishing good insulating characteristics.

The $C-V$ measurements were conducted on MFS capacitors to analyze the nature of the CBN/Si interface. Figure

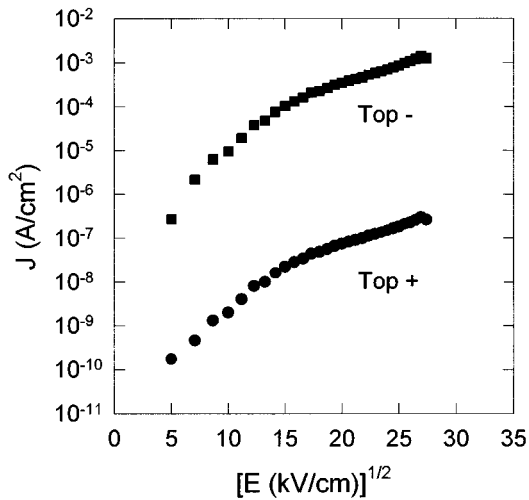


FIG. 3. Typical $J-E$ characteristic curve for the MFS structure using the highly oriented $\text{CaBi}_2\text{Nb}_2\text{O}_9$ thin films.

4 shows a typical $C-V$ hysteresis curve for Pt/CBN/Si capacitor with c -axis oriented CBN ferroelectric thin film. The $C-V$ measurements were conducted by applying a small ac signal of 10 mV amplitude and 100 kHz frequency while the dc electric field was swept from a negative bias to a positive bias and back again. The curve clearly shows the regions of accumulation, depletion, and inversion, and the clockwise direction of the curve reveals that the MFS capacitor structure had a good ferroelectric polarization switching property. The injection type on/off switching behavior or the ferroelectric polarization switching behavior can be established by the round trip direction of the hysteresis loop of the capacitance-voltage response. A clockwise rotation in the $C-V$ characteristic of a ferroelectric film on p -type Si is expected when charge compensation on the Si surface is induced by the polarization present in the film. This mode of switching is

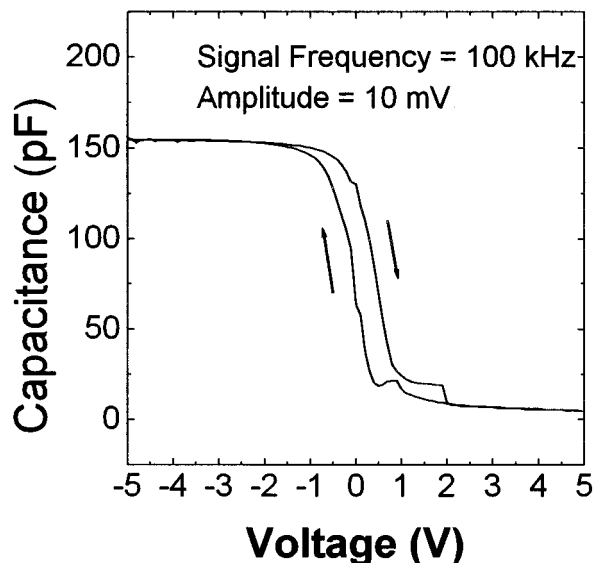


FIG. 4. Typical $C-V$ hysteresis curve for the MFS structure using the high oriented $\text{CaBi}_2\text{Nb}_2\text{O}_9$ thin films.

the desired mode for memory operation. An accumulation layer appeared at negative bias voltages since the ferroelectric film was deposited on p -type silicon substrate. The capacitance approached a maximum C_{\max} in the accumulation region corresponding approximately to the capacitance of the CBN thin film. The dielectric constant of the CBN thin films calculated from C_{\max} was 80. The dissipation factor was 0.051 at 100 kHz frequency. The flatband voltage was slightly shifted toward positive voltage, which may be due to built-in immobile charges associated with ionic defects in the ferroelectric thin film. As the applied voltage was increased and became positive, a depletion layer was formed inside silicon near the interface. A further increase in voltage caused inversion of the surface. The capacitance approached a minimum value C_{\min} in the inversion region. The measured minimum capacitance C_{\min} was 4.79 pF. The depletion capacitance C_D calculated from relation (1) using experimental values of C_{\max} and C_{\min} was 4.94 pF, and the theoretical value of C_D calculated from relation (2), was 5.13 pF.

$$1/C_{\min} = 1/C_{\max} + 1/C_D \quad (1)$$

and

$$C_D = \epsilon_s A / W_m, \quad (2)$$

where ϵ_s is the permittivity of silicon, A is the area of electrodes, and W_m is the maximum depletion width which was estimated to be 1.10 nm from the semiconductor data.⁷ The measured depletion capacitance was very close to the theoretical value, indicating that the film capacitance was not masked by any possible interface capacitance present in series with the film capacitance.

In summary, highly c -axis oriented $\text{CaB}_2\text{Nb}_2\text{O}_9$ thin films were successfully deposited directly on Si(100) by a pulsed laser deposition technique, and their MFS capacitor structure exhibited reasonable dielectric constant, low leakage current density, and a good ferroelectric polarization type switching property which is the desired mode for memory devices.

The authors wish to thank Masaya Nagata, Y. Zhu, X. Zhang, Dr. Y. S. Hwang, and Dr. D. P. Vijay for their invaluable help, and also would like to acknowledge the Korea Science and Engineering Foundation and SHARP Corp., Japan for funding this project.

¹ *Ferroelectric Thin Films V*, edited by S. B. Desu, R. Ramesh, B. A. Tuttle, R. E. Jones, and I. K. Yoo (1996), Vol. 433.

² S. Sinharoy, H. Buhay, D. R. Lampe, and M. H. Francombe, *J. Vac. Sci. Technol. A* **10**, 1554 (1992).

³ G. A. Smolenskii, V. A. Bokov, V. A. Isupov, N. N. Krainik, R. E. Pasynkov, and A. I. Sokolov, *Ferroelectrics and Related Materials*, edited by G. A. Smolenskii (Gordon and Breach Science Publishers, New York, 1984), Chap. 15.

⁴ D. B. Fenner, D. K. Biegelsen, and R. D. Bringans, *J. Appl. Phys.* **66**, 419 (1989).

⁵ G. V. Gibbs, M. B. Boisen, Jr., R. T. Downs, and K. L. Bartelmehs (XPOWLOT version 2.0) (1993).

⁶ R. E. Newnham, R. W. Wolfe, R. S. Horsey, F. A. Diaz-Coln, and M. I. Kay, *Mater. Res. Bull.* **8**, 1183 (1973).

⁷ H. F. Wolf, *Silicon Semiconductor Data* (Pergamon, New York, 1969).